Spin-Orbit Suppression of Cold Inelastic Collisions of Aluminum and Helium

Colin Bryant Connolly,[1,3] Yat Shan Au,[1,3] Eunmi Chae,[1,3] Timur V. Tscherbul,[3,4,5] Alexei A. Buchachenko,[6,7] Hsin-I Lu,[3,8] Wolfgang Ketterle,[2,3] and John M. Doyle[1,3]

[1]*Department of Physics, Harvard University, Cambridge, Massachusetts 02138, USA*
[2]*Department of Physics, MIT, Cambridge, Massachusetts 02139, USA*
[3]*Harvard-MIT Center for Ultracold Atoms, Cambridge, Massachusetts 02138, USA*
[4]*Institute for Theoretical Atomic, Molecular, and Optical Physics, Harvard-Smithsonian Center for Astrophysics, Cambridge, Massachusetts 02138, USA*
[5]*Chemical Physics Theory Group, Department of Chemistry, University of Toronto, Toronto, Ontario M5S 3H6, Canada*
[6]*Department of Chemistry, M. V. Lomonosov Moscow State University, Moscow 119991, Russia*
[7]*Institute of Problems of Chemical Physics, RAS, Chernogolovka, Moscow District 142432, Russia*
[8]*School of Engineering and Applied Sciences, Harvard University, Cambridge, Massachusetts 02138, USA*

(Received 31 August 2012; published 23 April 2013)

We present a quantitative study of suppression of cold inelastic collisions by the spin-orbit interaction. We prepare cold ensembles of $>10^{11}$ Al($^2P_{1/2}$) atoms via cryogenic buffer-gas cooling and use a single-beam optical pumping method to measure their magnetic (m_J-changing) and fine-structure (J-changing) collisions with ^{3}He atoms at millikelvin temperatures over a range of magnetic fields from 0.5 to 6 T. The experimentally determined rates are in good agreement with the functional form predicted by quantum scattering calculations using *ab initio* potentials. This comparison provides direct experimental evidence for a proposed model of suppressed inelasticity in collisions of atoms in $^2P_{1/2}$ states [T. V. Tscherbul *et al.*, Phys. Rev. A **80**, 040701(R) (2009)], which may allow for sympathetic cooling of other $^2P_{1/2}$ atoms (e.g., In, Tl and metastable halogens).

DOI: 10.1103/PhysRevLett.110.173202 PACS numbers: 34.50.−s, 34.20.Cf, 37.10.De

Introduction.—The expansion of the field of cold and ultracold atomic physics into systems beyond the alkali metals has led to the discovery of new physical phenomena, such as strongly dipolar quantum gases [1–4] and interaction anisotropy shielding in cold collisions [5–7], and to the development of interesting applications such as improved optical frequency standards [8–10] and quantum simulation schemes [11,12]. Collisions play a critical role in much of this research, being responsible for few-body interactions, thermalization, trap loss and decoherence. Theoretical guidance is crucial to understanding collisions; likewise, experiments provide the necessary tests for the validation of theoretical approaches. So far, few quantitative comparisons have been made between theory and experiment. Here we present such a comparison, providing definitive verification of a theory of suppressed inelastic collisions.

Inelastic collisions that reorient the atomic angular momentum are usually slow for atoms in S states, due to the spherical symmetry of the charge distribution, and fast for atoms in non-S states. However, it has recently been predicted that spin-orbit (SO) coupling in ^2P states can dramatically suppress those inelastic collisions [13], since in the $^2P_{1/2}$ state the precession of the orbital angular momentum leads to a spherical charge distribution. Inelastic transitions can still occur due to mixing of fine-structure states during a collision, but this mixing is suppressed by the SO splitting between the states, Δ_{SO}. In this Letter, we experimentally study this mechanism and quantitatively validate its theoretical description.

Theoretical quantum calculations based on *ab initio* interatomic potentials have had some recent success in predicting inelastic collision rates [7,14,15]. In many atomic systems, however, the collision rates are either too fast or too slow to be directly measured, which limits the range over which the theories can be tested. In one such case, the recent theory describing suppressed inelastic collisions of atoms in $^2P_{1/2}$ states (e.g., Al, Ga, In, and Tl, and metastable halogens) with He was supported by experiments done in tandem that observed large suppression in both Ga and In [13], but the very low rate constant for m_J-changing collisions (a critical process for magnetic trapping) was only bounded in both cases—not directly measured—leaving the test of theory incomplete.

In this work we study SO suppression of inelastic collisions between Al(^2P) and ^{3}He below 1 K. The SO interaction is of critical importance to cold collisions of many atomic species [16–19], and Al-He is an archetypal system for quantitative comparison between theory and experiment. In this system the SO interaction only partially suppresses inelasticity—much less so than with Ga and In—placing the inelastic rates within the dynamic range of experiment. We present here a combined experimental and theoretical study demonstrating this suppression and its magnetic field dependence, and obtain good agreement between our measurement and *ab initio* theory.

Using optical pumping, we investigate collisions that reorient the magnetic moment of the ground $^2P_{1/2}$ state (m_J-changing), and also collisions that cause fine-structure relaxation from the $^2P_{3/2}$ state to the ground state (J-changing). Compared to previous work with $^2P_{1/2}$ atoms [13], our experiment is performed at a much lower temperature and over a range of much higher magnetic fields, at a scale relevant for magnetic trapping.

Experiment.—We measure the inelastic m_J-changing and J-changing collision rates of Al colliding with a cryogenic ^{3}He buffer gas using an optical pumping method that employs a single pump-probe laser. The competition between optical pumping and collisional refilling produces a steady-state population within $\approx$1 ms, which we monitor via the optical depth (OD, calculated from pump laser absorption). We observe the OD while changing both the pump power and ^{3}He density so as to vary the optical pumping and collision rates independently and extract the inelastic collision rate constants. Our experiment is sensitive to both m_J- and J-changing collisions because the two ground-state sublevels experience different refilling rates, and we make separate measurements with the pump laser resonant with one or the other sublevel.

Atoms are held inside a cell maintained at a temperature of 820 mK [20]. A superconducting Helmholtz pair of magnet coils surrounds the cell to apply homogeneous fields of up to 6 T. We produce $>10^{11}$ cold Al atoms by Nd:YAG laser ablation of an AlN ceramic target into a ^{3}He buffer gas. After cooling to the cell temperature, the Al atoms slowly diffuse to the walls of the cell, where they freeze; our optical pumping measurements take place as the atoms diffuse.

The energy level diagram for Al in a magnetic field is shown in Fig. 1. The optical pumping laser is tuned to the 394.5-nm ground state transition ($^2P_{1/2} \rightarrow {}^2S_{1/2}$) and can be made resonant either with the low- or high-field-seeking (LFS or HFS) magnetic sublevel. The excited state spontaneously decays with 22% probability back to the original resonant state and with 11% and 66% probability to the opposite $^2P_{1/2}$ magnetic sublevel and to the upper $^2P_{3/2}$ manifold, respectively [21]. Only atoms with nuclear spin projection $m_I = 5/2$ are addressed by the pump laser; the nuclear spin exchange rate in cold collisions of atoms with ^{3}He is in general very low [22,23], so atoms in other nuclear spin states do not participate. The atoms that spontaneously decay to the ground state HFS sublevel can return to the LFS sublevel via m_J-changing collisions that reorient the Al magnetic moment. Atoms in the upper manifold can lose angular momentum in J-changing collisions to make transitions to either sublevel of the $^2P_{1/2}$ manifold. The anisotropy of the $^2P_{3/2}$ state ensures that rapid m_J-changing collisions within that manifold will rapidly transfer population to the lowest-energy sublevel [13], and so $m_J > -3/2$ sublevels of that state are neglected.

Diffusion of atoms into and out of the laser beam can also compete with optical pumping. At low ^{3}He density, atoms pumped to other states will rapidly diffuse out of the beam and be replaced with "unpumped" atoms (in the resonant state) diffusing in. Hence the observed OD increases with falling ^{3}He density in the low-density regime. At high ^{3}He density, diffusion is slow and does not affect OD.

The rate equations describing the system when the pump laser is resonant with the LFS sublevel are given by

$$\dot{N}_+(\boldsymbol{r}, t) = -\Gamma_p(1 - C_+)N_+ + \Gamma_m(\kappa N_- - N_+) + f_+\Gamma_J N_{3/2} + D\nabla^2 N_+, \quad (1)$$

$$\dot{N}_-(\boldsymbol{r}, t) = \Gamma_p C_- N_+ - \Gamma_m(\kappa N_- - N_+) + f_-\Gamma_J N_{3/2} + D\nabla^2 N_-, \quad (2)$$

$$\dot{N}_{3/2}(\boldsymbol{r}, t) = \Gamma_p C_{3/2} N_+ - \Gamma_J N_{3/2} + D\nabla^2 N_{3/2}. \quad (3)$$

N_X is the spatially and temporally varying population of state X. The indices $+$, $-$, and $3/2$ refer to the LFS and HFS sublevels of the ground state and to the $m_J = -3/2$ sublevel of the $^2P_{3/2}$ manifold, respectively. Γ_p, Γ_m and Γ_J are the rates of optical pumping, m_J-changing collisions and J-changing collisions, respectively, and D is the diffusion constant for Al in ^{3}He. The coefficients C_X and f_X are the branching fractions into state X for spontaneous emission from the $^2S_{1/2}$ state and for J-changing transitions from the $^2P_{3/2}$ state, respectively. The Boltzmann factor κ suppresses transitions to higher-energy magnetic sublevels and is given by $\kappa = \exp(-g_J\mu_B B/k_B T)$ for atoms at temperature T in a magnetic field B, where

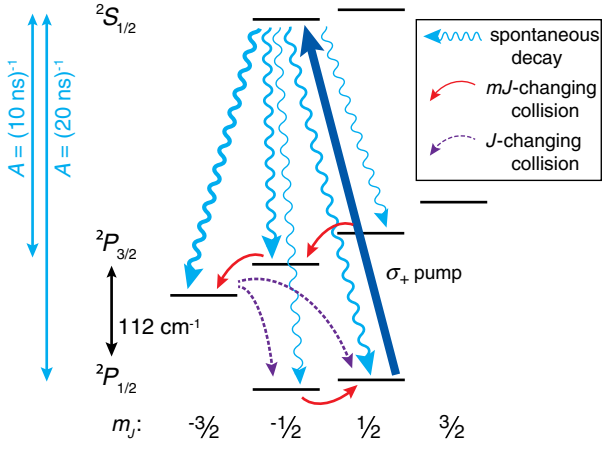

FIG. 1 (color online). Energy level diagram of Al with relevant state-changing processes for the case of optical pumping of the $m_J = +1/2$ LFS state.

$g_J = 2/3$ is the Landé g factor, μ_B is the Bohr magneton, and k_B is the Boltzmann constant.

The helium density is characterized by monitoring diffusion of Al to the walls of the cell. The diffusion time τ_d is given by $\tau_d = (n_b \sigma_d)/(\bar{v} G)$, where n_b is the buffer gas density, σ_d is the thermally averaged momentum transfer cross section, $\bar{v} = (8 k_B T/\pi\mu)^{1/2}$ is the mean Al-^{3}He collision velocity with reduced mass μ, and $G \approx 0.22$ cm^{-2} is a geometric factor describing the cylindrical cell of radius ≈ 3 cm. τ_d is proportional to the Al-^{3}He collision rate, and hence also to the inelastic transition rates Γ_m and Γ_J, i.e.,

$$\Gamma_m = n_b k_m = \frac{n_b \sigma_d \bar{v}}{\gamma_m} = \left(\frac{\bar{v}^2 G}{\gamma_m}\right)\tau_d, \quad (4)$$

$$\Gamma_J = \left(\frac{\bar{v}^2 G}{\gamma_J}\right)\tau_d, \quad (5)$$

where γ_m and γ_J are the ratios of the ground-state momentum transfer rate to the inelastic m_J- and J-changing collision rates. Expressing the inelastic rates in this manner decouples the measurement of γ_m and γ_J from uncertainty in calibrating n_b.

The solution of Eqs. (1)–(3) is nontrivial due to the spatial dependence of diffusion. However, in the range of parameters relevant to the experiment, the dependence of OD on the pump power P is well approximated by the model function

$$\mathrm{OD} = a\left(\frac{1-c}{bP+1} + c\right), \quad (6)$$

where a is the OD at vanishing pump power and b increases with the rate of relaxation and diffusion. Equation (6) is an exact solution for $D = 0$ and only homogeneous broadening, with $c = 0$ and $b \propto \Gamma_p/\Gamma_m$. Magnetic field inhomogeneity introduces a dependence on the Zeeman-broadened line shape and is addressed with the parameter c, which grows with increasing linewidth (generally $c < 0.1$). Additionally, if $D > 0$ then the form of b is complicated at low helium density. We have verified numerically that these effects do not significantly alter the extracted parameters.

The exact experimental procedure is as follows: We retroreflect the circularly polarized pump laser with diameter ≈ 4 mm from a mirror in the cell, passing through the atoms twice, propagating parallel to the magnetic field. We modulate the pump power over a range of four logarithmically spaced powers from 0.3–30 μW, pausing for 3 ms at each power level to allow the Al state distribution to stabilize. The saturation parameter is $<1\%$ at all power levels. Many periods of the power modulation cycle occur during the Al diffusive lifetime, and we collate the observed OD by power level into four data sets that we individually fit to diffusive decay of the form $\mathrm{OD} = \mathrm{OD}_0 \exp(-t/\tau_d)$ with a shared τ_d. Finally, we fit the resulting four values of OD_0 to the model function in Eq. (6). The process is repeated over a range of ^{3}He densities and magnetic fields to map out the optical pumping response. An example for $B = 4$ T is shown in Fig. 2.

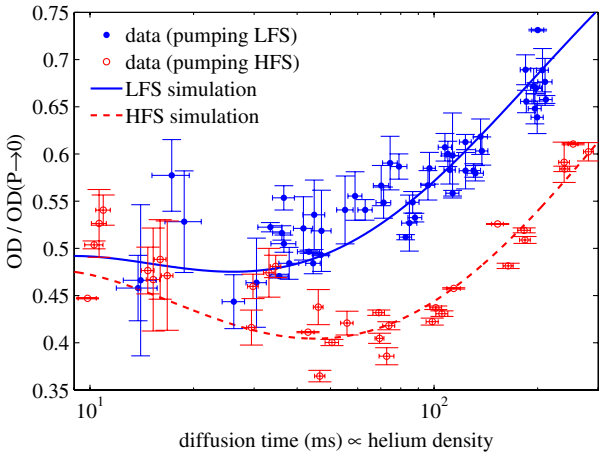

FIG. 2 (color online). Al optical pumping data taken at $T = 820$ mK and $B = 4$ T. Each data point is a separate realization of the experiment. The quantity plotted is the ratio of predictions from the model function fit [Eq. (6)] for the optical depth (OD) observed at an arbitrary pump power P (same for all points) to the low-power limit ($P \to 0$). Since OD is suppressed by optical pumping, this quantity ranges from 0 (complete resonant state depletion) to 1 (no perturbation). Data are plotted for a pump laser resonant with either the LFS (blue closed circles) or HFS (red open circles) state, as well as best-fit simulated curves.

Analysis.—To determine the inelastic collision rate constants, we solve Eqs. (1)–(3) numerically and perform least-squares fits of the data to the simulation. The free parameters are the inelastic collision ratios γ_m and γ_J and the branching fraction $f_+ = 1 - f_-$ for J-changing transitions from the upper fine structure state to the ground $m_J = +1/2$ sublevel. In addition, a pump beam power scaling factor of $\lesssim 2$ is included as a free parameter to account for imperfect knowledge of experimental parameters to which the numerical simulation is sensitive.

Allowing the branching fraction f_+ to vary freely between 0 and 1 in the fit introduces a systematic bias toward finding $\gamma_m \sim \gamma_J$. To address this bias, we perform separate fits using two fitting procedures (Fig. 3), one in which the branching fraction f_+ is unbounded, and another fixing f_+ to an *a priori* theoretical value of 0.716 (see Supplemental Material [24] for detailed explanation and derivation of this value). For all fits, a bootstrapping procedure is used to estimate confidence intervals for the best-fit parameters.

Theoretical calculations.—We use the rigorous quantum scattering formalism [13,25] to describe the quantum dynamics of cold collisions of ^2P atoms in a magnetic field. The Hamiltonian for the $M(^2P)$-He complex may be written in atomic units as

$$\hat{H} = -\frac{1}{2\mu R}\frac{\partial^2}{\partial R^2}R + \frac{\hat{\ell}^2}{2\mu R^2} + \hat{H}_M + \hat{V}(\mathbf{R}, \mathbf{r}), \quad (7)$$

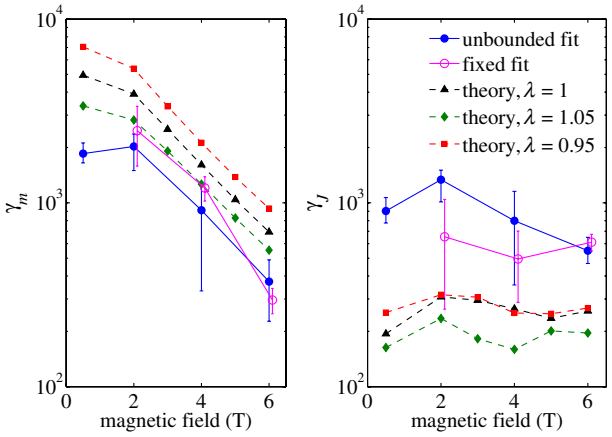

FIG. 3 (color online). Theoretical (dashed lines) and experimental (solid lines) results for the momentum-transfer-to-inelastic collision ratios γ_m and γ_J at $T = 820$ mK. Theoretical values are calculated from the Al(^2P)-He potentials scaled by a factor λ. Experimental values are best-fit parameters obtained from least-squares fitting of optical pumping data to numerical simulation of Eqs. (1)–(3). Fitting is performed both with the J-changing collision branching fraction f_+ unbounded (blue closed circles) and with $f_+ = 0.716$ (magenta open circles). The latter are horizontally offset by 0.1 T for clarity.

where μ is the reduced mass, R is the interatomic distance, $\mathbf{r}$ denotes the electronic coordinates, and $\hat{\ell}$ is the rotational angular momentum of the nuclei. The operator $\hat{H}_M = A_{\rm SO}\hat{L}\cdot\hat{S} + \mu_{\rm B}B(\hat{L}_z + 2\hat{S}_z) + \hat{H}_I$ is the Hamiltonian of the isolated atom M in magnetic field B and the operator $\hat{V}(\mathbf{R}, \mathbf{r})$ is the M-He interaction potential. $A_{\rm SO} = \frac{2}{3}\Delta_{\rm SO}$ is the spin-orbit constant of atom M ($\Delta_{\rm SO} = 112$ cm^{-1} for Al). $\hat{L}_z$ and $\hat{S}_z$ are the projections of the electronic orbital angular momentum and spin operators $\hat{L}$ and $\hat{S}$ onto the magnetic field axis, and $\hat{H}_I$ is the hyperfine Hamiltonian [13]. The wave function of the collision complex is expanded in the fully-uncoupled $|Jm_J\rangle|Im_I\rangle|\ell m_\ell\rangle$ basis [13,25] and inserted into the Schrödinger equation with the Hamiltonian in Eq. (7) to yield a system of close-coupled equations that are solved to obtain probabilities for collision-induced Zeeman transitions of the form $|J, m\rangle \rightarrow |J', m'\rangle$ as functions of collision energy and magnetic field ($m = m_J + m_I$).

To parameterize the close-coupled equations, we use the accurate *ab initio* interaction potentials for Al-He of Σ and Π symmetry from Ref. [26], fitted to analytic functions with proper long-range behavior. To obtain the ground-state momentum transfer rate, $k_{\rm d}$, we solve a one-dimensional scattering problem based on the lowest spin-orbit-coupled potential $V_{1/2,1/2}(R)$ obtained by diagonalizing a 3×3 Hamiltonian matrix [27]. We find that this approximation reproduces the exact multichannel elastic rate, which has only weak magnetic field dependence in this range, to within 10% over the temperature range 0.1–2 K (including scattering resonances). At 820 mK we calculate $k_{\rm d} = 3.6\times 10^{-10}$ cm^3/s. Dividing the momentum transfer rate by the appropriate Zeeman relaxation rates yields the collision ratio γ for each inelastic process: γ_m includes only inelastic transitions of the form $|J, m_J\rangle \rightarrow |J, -m_J\rangle$, where $J = 1/2$; and γ_J includes inelastic transitions of the form $|J = 3/2, m_J = -3/2\rangle \rightarrow |J' = 1/2, m'_J = \pm 1/2\rangle$, since only the lowest-energy sublevel of the $^2P_{3/2}$ manifold is significantly populated in the experiment. The nuclear spin state is $m_I = I = 5/2$ for all calculations.

The calculated values of γ_m and γ_J are shown in Fig. 3. Despite the much smaller SO splitting in Al compared to Ga and In, Zeeman relaxation remains strongly suppressed in the $^2P_{1/2}$ ground state. In addition, the approximate magnetic field dependence of the m_J-changing collision rate at high field follows the scaling predicted from first-order perturbation theory due to the admixture of the upper fine-structure state into the ground $^2P_{1/2}$ state,

$$|\tilde{J}m_J\rangle = |J = 1/2, m_J\rangle + \beta|J = 3/2, m_J\rangle, \qquad (8)$$

where $\beta = (\sqrt{2}/3)(\mu_{\rm B}B/\Delta_{\rm SO})$. The Zeeman relaxation cross section is given to first order by the square of the matrix element of the interaction potential $\hat{V}(\mathbf{R}, \mathbf{r})$ between the wave functions given by Eq. (8) with $m_J = +1/2$ and $-1/2$. Therefore, $k_m \propto \beta^2$ and hence we expect $\gamma_m \propto B^{-2}$. Fitting a power-law function ($\gamma_m \propto B^p$) to the results of the multichannel scattering calculation of the ratio γ_m for $B \geq 3$ T gives an exponent $p = -1.85$.

For direct comparison to the theoretical calculations, we use the experimental results obtained by fitting the data with fixed branching fraction, which provides better agreement over the range $B = 2$ to 6 T. We explore the sensitivity of our calculations to the interatomic potential by repeating the calculation with both the V_Σ and V_Π potentials scaled by $\lambda = 0.95$ and 1.05. The calculated rate of m_J-changing collisions increases with λ (Fig. 3) due to the increased interaction anisotropy. We find good agreement between the measured and calculated dependence on magnetic field for both γ_m and γ_J. The values of γ_m are in better agreement for $\lambda = 1.05$, which is consistent with the fact that the *ab initio* calculations [26] underestimate the interaction strength. The magnitude of the measured and calculated values of γ_J differ by about a factor of two, with no clear improvement evident using the scaled potentials.

Conclusion.—We measure significant SO suppression of m_J- and J-changing collision rates in the Al(^2P)-^{3}He system at 820 mK and find good agreement with quantum scattering calculations using *ab initio* potentials. The magnetic field dependence at high fields is well reproduced for both processes, providing direct evidence for the theoretical model [13].

For future studies with ^2P atoms, we note that the much larger SO splittings for In, Tl, and the metastable halogens Br and I ($\Delta_{\rm SO} = 2213$, 7793, 3685 and 7603 cm^{-1},

respectively [28]) lead to much stronger suppression of inelastic transitions of those atoms with He [13]. Our work demonstrates that this suppression also holds at the large magnetic fields necessary for trapping, implying that sympathetic cooling with magnetically trapped S-state atoms may be possible, provided that the ratio of the interaction anisotropy to Δ_{SO} is sufficiently small. Preliminary calculations show that this is the case for spin-polarized interactions of Tl with heavy alkali or light alkaline earth atoms—especially the Tl-Mg system, for which this ratio is similar to that of Al-He. This may provide a robust source of ultracold ^2P atoms for many-body physics with SO interactions and precision measurements of electric dipole moments [29]. The halogen species are particularly appealing for the study of cold collisions and chemical reactions [30], and of radiative properties of the metastable $^2P_{1/2}$ states.

This work was supported by the NSF under Grant No. PHY-1067990 and through the Harvard/MIT Center for Ultracold Atoms, and by RFBR under Project No. 11-03-00081.

[1] J. Stuhler, A. Griesmaier, T. Koch, M. Fattori, T. Pfau, S. Giovanazzi, P. Pedri, and L. Santos, Phys. Rev. Lett. **95**, 150406 (2005).
[2] M. Lu, N. Q. Burdick, S. H. Youn, and B. L. Lev, Phys. Rev. Lett. **107**, 190401 (2011).
[3] M. Lu, N. Q. Burdick, and B. L. Lev, Phys. Rev. Lett. **108**, 215301 (2012).
[4] K. Aikawa, A. Frisch, M. Mark, S. Baier, A. Rietzler, R. Grimm, and F. Ferlaino, Phys. Rev. Lett. **108**, 210401 (2012).
[5] C. I. Hancox, S. C. Doret, M. T. Hummon, L. Luo, and J. M. Doyle, Nature (London) **431**, 281 (2004).
[6] C. I. Hancox, S. C. Doret, M. T. Hummon, R. V. Krems, and J. M. Doyle, Phys. Rev. Lett. **94**, 013201 (2005).
[7] R. V. Krems, J. Kłos, M. F. Rode, M. M. Szczęśniak, G. Chałasiński, and A. Dalgarno, Phys. Rev. Lett. **94**, 013202 (2005).
[8] C. Oates, F. Bondu, R. Fox, and L. Hollberg, Eur. Phys. J. D **7**, 449 (1999).
[9] M. M. Boyd, A. D. Ludlow, S. Blatt, S. M. Foreman, T. Ido, T. Zelevinsky, and J. Ye, Phys. Rev. Lett. **98**, 083002 (2007).
[10] N. D. Lemke, A. D. Ludlow, Z. W. Barber, T. M. Fortier, S. A. Diddams, Y. Jiang, S. R. Jefferts, T. P. Heavner, T. E. Parker, and C. W. Oates, Phys. Rev. Lett. **103**, 063001 (2009).
[11] A. V. Gorshkov, A. M. Rey, A. J. Daley, M. M. Boyd, J. Ye, P. Zoller, and M. D. Lukin, Phys. Rev. Lett. **102**, 110503 (2009).
[12] A. V. Gorshkov, M. Hermele, V. Gurarie, C. Xu, P. S. Julienne, J. Ye, P. Zoller, E. Demler, M. D. Lukin, and A. M. Rey, Nat. Phys. **6**, 289 (2010).
[13] T. V. Tscherbul, A. A. Buchachenko, A. Dalgarno, M.-J. Lu, and J. D. Weinstein, Phys. Rev. A **80**, 040701 (2009).
[14] A. A. Buchachenko, Y. V. Suleimanov, M. M. Szczęśniak, and G. Chałasiński, Phys. Scr. **80**, 048109 (2009).
[15] T. V. Tscherbul, J. Kłos, A. Dalgarno, B. Zygelman, Z. Pavlovic, M. T. Hummon, H.-I. Lu, E. Tsikata, and J. M. Doyle, Phys. Rev. A **82**, 042718 (2010).
[16] S. E. Maxwell, M. T. Hummon, Y. Wang, A. A. Buchachenko, R. V. Krems, and J. M. Doyle, Phys. Rev. A **78**, 042706 (2008).
[17] B. Zygelman and J. D. Weinstein, Phys. Rev. A **78**, 012705 (2008).
[18] A. Yamaguchi, S. Uetake, D. Hashimoto, J. M. Doyle, and Y. Takahashi, Phys. Rev. Lett. **101**, 233002 (2008).
[19] A. Traverso, R. Chakraborty, Y. N. Martinez de Escobar, P. G. Mickelson, S. B. Nagel, M. Yan, and T. C. Killian, Phys. Rev. A **79**, 060702 (2009).
[20] C. B. Connolly, Ph.D. thesis, Harvard University, 2012.
[21] D. E. Kelleher and L. I. Podobedova, J. Phys. Chem. Ref. Data **37**, 709 (2008).
[22] T. V. Tscherbul, P. Zhang, H. R. Sadeghpour, A. Dalgarno, N. Brahms, Y. S. Au, and J. M. Doyle, Phys. Rev. A **78**, 060703 (2008).
[23] T. V. Tscherbul, P. Zhang, H. R. Sadeghpour, and A. Dalgarno, Phys. Rev. Lett. **107**, 023204 (2011).
[24] See Supplemental Material at http://link.aps.org/supplemental/10.1103/PhysRevLett.110.173202 for a discussion of the fitting procedure with fixed branching fraction, f_+.
[25] R. V. Krems and A. Dalgarno, Phys. Rev. A **68**, 013406 (2003).
[26] H. Partridge, J. R. Stallcop, and E. Levin, J. Chem. Phys. **115**, 6471 (2001).
[27] V. Aquilanti, G. Liuti, F. Pirani, and F. Vecchiocattivi, J. Chem. Soc., Faraday Trans. 2 **85**, 955 (1989).
[28] A. Kramida, Yu. Ralchenko, J. Reader, and (NIST ASD Team), NIST Atomic Spectra Database, version 4.1, 2012, http://physics.nist.gov/asd.
[29] B. K. Sahoo, R. Pandey, and B. P. Das, Phys. Rev. A **84**, 030502 (2011).
[30] R. V. Krems, Phys. Chem. Chem. Phys. **10**, 4079 (2008).